

Synthesis of amino-containing oligophenylsilsesquioxanes

S.G. Kim, J. Choi, R. Tamaki, Richard M. Laine*

Departments of Chemistry, and Materials Science and Engineering, and the Macromolecular Science and Engineering Center, University of Michigan, 2114, H.H. Dow Building, 2300 Hayward, Ann Arbor, MI 48109-2136, USA

Available online 23 March 2005

This contribution is in honor of Professor James Marks' 70th birthday and all of his exceptional contributions to silane chemistry.

Abstract

A series of aminophenylsilsesquioxanes were prepared from octaphenylsilsesquioxane (OPS), dodecaphenylsilsesquioxane (DPS) and two polyphenylsilsesquioxanes, one a low molecular weight LMW oligomer (PPS) and the other a high molecular weight (HMW) PPS (M_n of 1.3×10^3 , PPS) and two polyhedral materials. LMS and HMW PPS were obtained by polycondensation of $\text{PhSi}(\text{OEt})_3$ to form oligomeric, incompletely-condensed frameworks. The oligomer was used as is for nitration to produce LMW polynitrophenylsilsesquioxane (PNPS). However, optimization of hydrolysis and condensation processes using KOH as catalyst, led to a route to HMW PPS (M_n of 2.5×10^4 , M_w of 6.1×10^4), which was best prepared in EtOH.

OPS, DPS, LMW PPS (M_n of 1.3×10^3), and HMW PPS (M_n of 2.5×10^4), were nitrated using 90% fuming HNO_3 , and then reduced using triethylamine, formic acid, and 5% Pd/C in THF. The products were characterized using ^1H , ^{13}C , and ^{29}Si NMR, GPC, FT-IR, and TGA. Amino groups (NH_2) were introduced primarily in *meta* and *ortho* positions in a 70:25 ratio with the remainder being *para*. It was determined that little or no OPS or DPS cage cleavage occurred coincident with nitration or reduction if the latter process was run at 40°C , whereas the MW of HMW PPS decreased to 1.6×10^3 after nitration and reduction. The M_n suggests that for both LMW and HMW PPS, the same PAPS product forms, which consists of monomer, dimer, and trimer species.

© 2005 Elsevier Ltd. All rights reserved.

Keywords: Nanocomposites; Silsesquioxanes; Polyaminophenylsilsesquioxanes

1. Introduction

Polyhedral cubic or octameric silsesquioxanes produced by hydrolytic condensation of trifunctional organosilicon monomers (RSiX_3) are attractive materials for numerous applications [1]. Since their discovery in 1946 [2], the chemistry and properties of these materials have been the subject of numerous studies. Recent efforts have focused on stoichiometrically well-defined cubic silsesquioxane frameworks, including a wide variety of frameworks with synthetically useful functional groups [3–9].

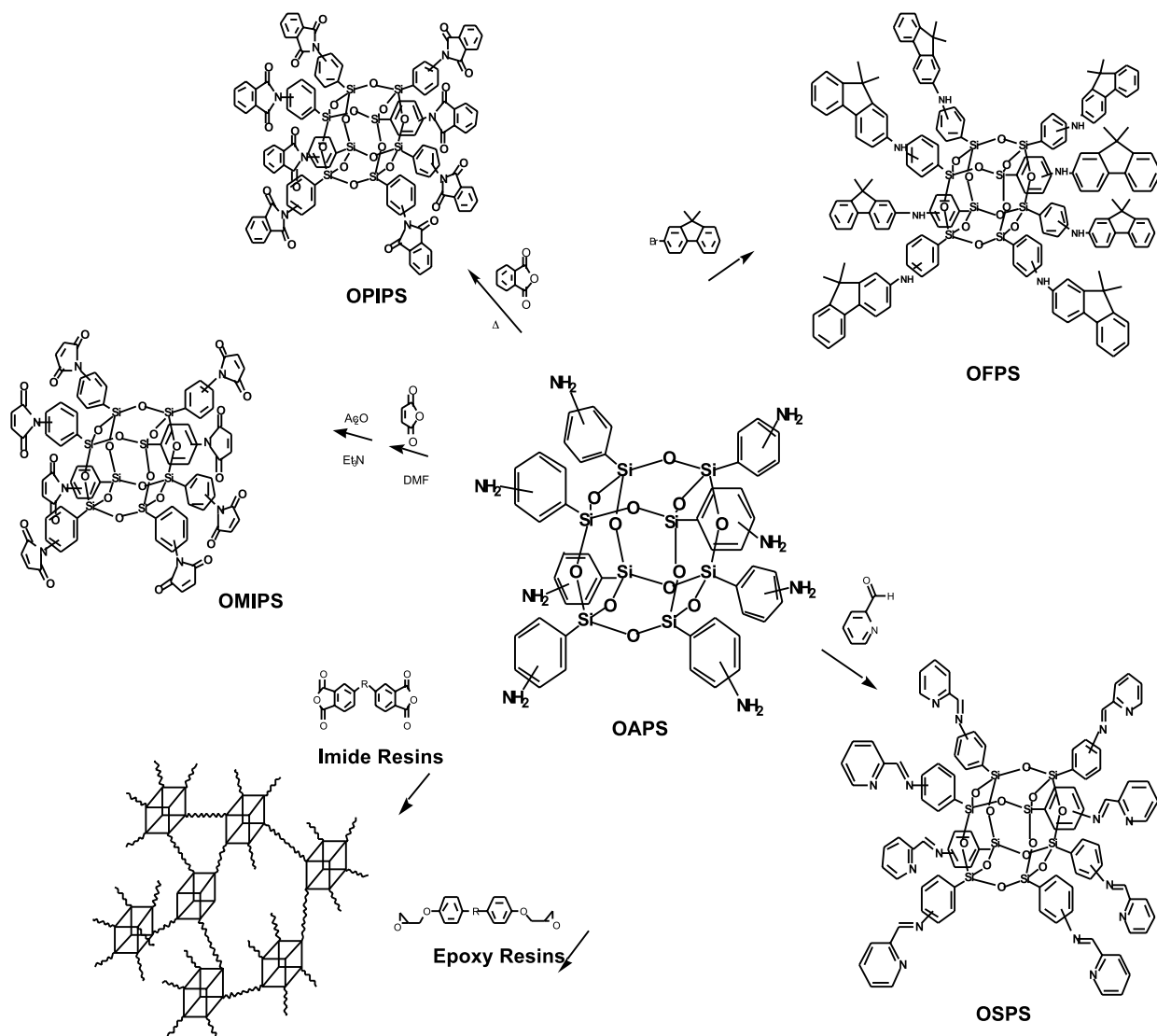
Among various silsesquioxanes, the octaphenylsilsesquioxane [OPS, $(\text{PhSiO}_{1.5})_8$], decaphenylsilsesquioxane [DPS, $(\text{PhSiO}_{1.5})_{10}$], dodecaphenylsilsesquioxane [DDPS, $(\text{PhSiO}_{1.5})_{12}$], and polyphenylsilsesquioxane (PPS) systems are among the most interesting because of their high

temperature stability ($> 500^\circ\text{C}$) [10]. Since the initial PPS syntheses [11–12], numerous efforts have been made to control polymer structure and properties using various methods to catalyze the hydrolysis of PhSiCl_3 , $\text{PhSi}(\text{OR})_3$ or related starting materials. Despite this, the actual structures remain poorly characterized [13–15] because their structures are often affected by a great number of synthetic variables imposed during preparation [14–15], many possible complex network structures and architectures can be envisioned to form. Scheme 1 shows several possibilities.

In recent years, PPS derivatives have been used as lithographic materials [16] gas-separation membranes [17], second-harmonic generators [18], insulators for semiconductor devices [10] silicon oxycarbide precursors [19], and carcinostatic drugs [20]. PPhS has also attracted widespread interest as a precursor to hybrid inorganic/organic materials and as comonomers for new families of silsesquioxane based polymers and as building blocks for solid networks [3,21–22].

Laine et al. recently described the synthesis of a variety of octafunctional compounds and their use in forming

* Corresponding author. Fax: +1 313 761 4788.



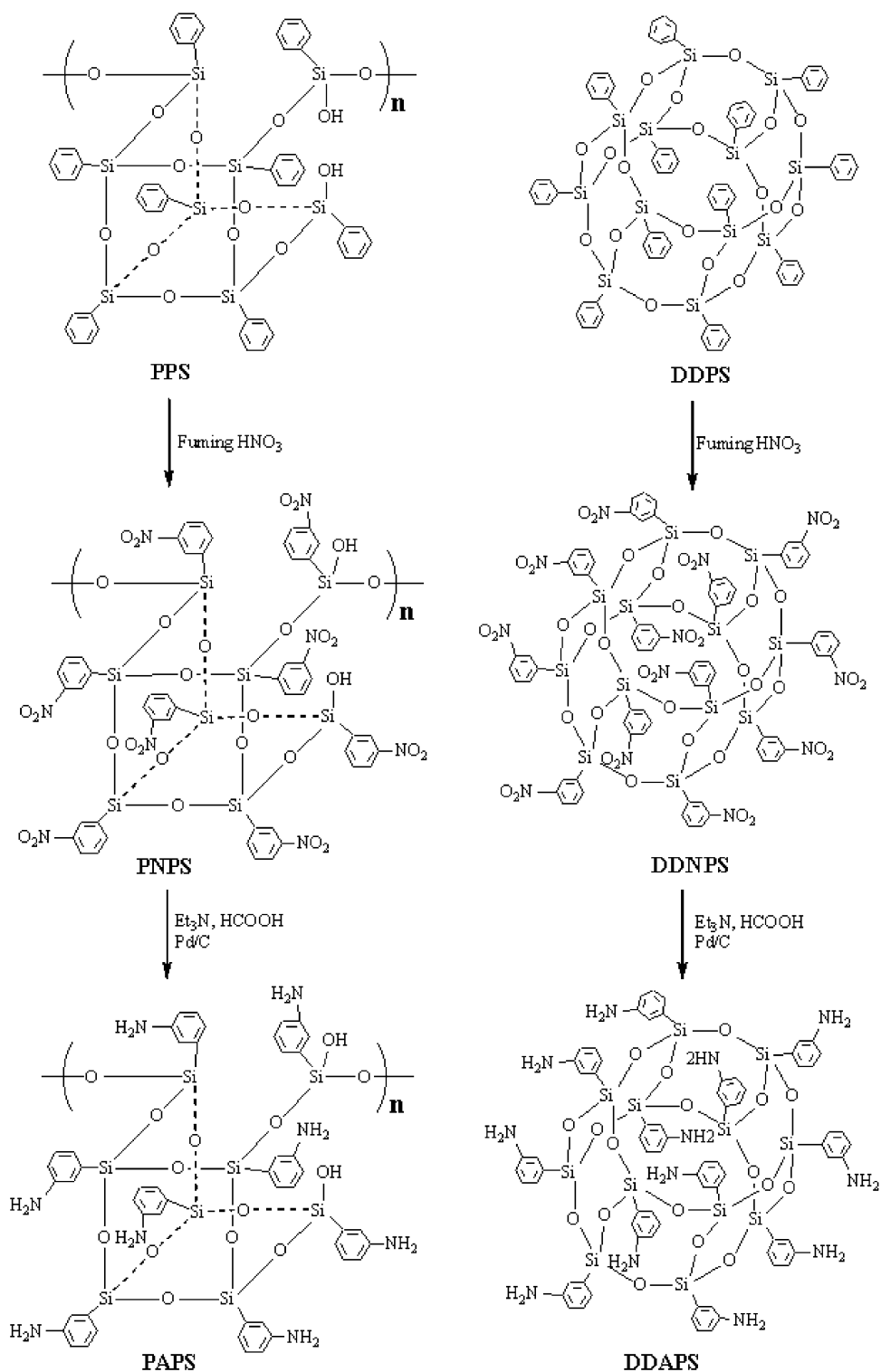
Scheme 1.

nanocomposites with high surface areas, unusual mechanical properties and high thermal stabilities [23–25]. The development of hybrid materials from cubic silsesquioxanes is a subject of intense research. Using polyfunctional silsesquioxanes, the synthesis of hybrid materials wherein the control of the size and shape of the organic and inorganic components becomes possible at the nanometer level, providing potential access to novel properties.

Recently, functionalized cubic silsesquioxanes were examined as potential building blocks for hybrid composites wherein the architecture and length of the organic tether between cubes could be completely defined. Octafunctional silsesquioxanes were obtained mostly by hydrosilylation of organic molecules having alkenyl [26] or alkynyl end groups [27–29]. However, the utility of these types of silsesquioxane materials are restricted by the flexible aliphatic chains that decrease the thermal and mechanical stability of nanocomposites based on these materials.

In an effort to overcome these problems, we recently reported the synthesis of the wholly aromatic octafunctional octa(aminophenyl)silsesquioxane (OAPS) cube [30]. This new organic/inorganic macromonomer provides access to nanocomposites for high temperature applications not only because OAPS possesses improved thermal stability, but also more importantly because various functional groups can be derived from the amine groups of OAPS cube providing limitless opportunities for manipulating/tailoring nanocomposite properties. Some examples of its reaction chemistry are shown in Scheme 1.

We present here an extension of the octaminophenyl work using poly(phenyl)silsesquioxane (PPS), and dodecaphenylsilsesquioxane (DDPS). We discuss the synthesis of dodeca(aminophenyl)silsesquioxane (DDAPS), and poly(aminophenyl)silsesquioxane (PAPS), which contain incompletely-condensed frameworks as, suggested below. (Scheme 2).



Scheme 2.

2. Experimental section

2.1. Materials

PPS starting material was obtained from Gelest Inc. The M_n and M_w of this material were determined by GPC to be

1.3×10^3 and 2.2×10^3 , respectively. This PPS was used as a calibration standard. It was ground to a powder and dried under vacuum at $70^\circ\text{C}/24\text{ h}$. DDPS was a gift from Hybrid Plastics Inc., and was also used as a starting material after drying under vacuum at $70^\circ\text{C}/24\text{ h}$. Reagents and reaction solvents were purified under N_2 as follows: tetrahydrofuran

(THF) and toluene were freshly distilled from a mixture of sodium/benzophenone ketyl before use. Methyl alcohol and ethyl alcohol were distilled before use. Nitric acid 90%, formic acid 99% and triethylamine were obtained from Aldrich and used without further purification. Also, 5% Pd/C, KOH, NaOH, ethyl acetate, tetrabutylammonium fluoride, and hexane were obtained from Aldrich and used without purification.

2.2. Characterization: NMR analysis

All ^1H - and ^{13}C -NMR analyses were run in acetone- d_6 and recorded on a Varian INOVA 400 spectrometer. ^1H -NMR spectra were collected at 400.0 MHz using a 6000 Hz spectral width, a relaxation delay of 2.67 s, a pulse width of 40° , 30 k data points, and acetone- d_6 (2.04 ppm) as internal reference. ^{13}C (^1H) NMR spectra were obtained at 100 MHz using a 25 KHz spectral width, a relaxation delay of 1.5 s, a pulse width of 40° , 75 k data points, and acetone- d_6 (77.23 ppm) as internal reference. All CP-MAS solid state NMR spectra were obtained at 9 T using a Chemagnetics CMX-400 spectrometer operating at 79.5 MHz for ^{29}Si and 400.13 MHz for ^1H . Contact times were 2 ms and pulse delays 20 s. The probe used was a Chemagnetics PENCIL design using 5 mm zirconia rotors at spinning rates of 3 kHz. The sample temperature was at 30°C and TMS referenced the chemical shifts.

2.2.1. Fourier transform infrared spectra (FTIR)

FTIR were recorded on a Mattson Galaxy Series 3020 bench adapted with a Harrick Scientific 'Praying Mantis' DR accessory (DRA-2CO). KBr was used as a nonabsorbent medium. Sample was ground with KBr to make a 1 wt% mixture and packed tightly in the sample holder. After the sample was loaded into the chamber, nitrogen was purged for about 10 min before data collection. A minimum of 32 scans was collected for each sample at a resolution of 4 cm^{-1} .

2.2.2. Thermal gravimetric analyses (TGA)

TGA were performed on a SDT 2960 simultaneous DTA-TGA thermogravimetric analyzer (TA instrument, Inc., New Castle, DE). The instrument was calibrated with Alumel and iron supplied by TA. Measurements were performed under a continuous flow of synthetic air (110 ml/min), at $10^\circ\text{C}/\text{min}$ to 1000°C .

2.2.3. Gel permeation chromatography (GPC)

GPC were performed on a Waters GPC system, using a Waters 410 RI detector and a Waters 486 UV detector, Waters Styragel columns (7.8×300 , HR 0.5, 1, 3, 4), and a PL-DCU data capture unit from Polymer Laboratory. The system was calibrated using polystyrene standards obtained from Polymer Laboratory. THF was used as the eluent, at a flow rate of 1.0 ml/min.

2.2.4. Synthesis of OPS with phenyltriethoxysilane (PTES)

PTES used as a starting material in this standard reaction. PTES, 7 g (29.1 mmol) was added to a flask equipped with a cooling condenser and a Dean-Stark system to remove distilled ethyl alcohol and water from the reaction solution. To this flask was added 50 ml EtOH, and then KOH (0.57 g, 7.5 wt% based on PTES). The solution was heated to refluxing temperature with stirring, and then water was added slowly (0.5 ml, 10 wt% based on PTES) in small portions over a 30 min period. After 3 h, a white powder began to be precipitate. The reactions were run for 40 h. After this time, the precipitated white powder (OPS) was filtered off, and washed 3 times with methyl alcohol (20 ml). The products were vacuum dried at $70^\circ\text{C}/7\text{ h}$. Yields were 90%. Selected characterization data are shown in Table 2.

2.2.5. Polymerization of oligomeric poly(phenyl)silsesquioxane (PPS)

To prepare high molecular weight PPS, precursor (low MW PPS; $M_n=1.3\times 10^3$) obtained from Gelest was polymerized in various solvents with KOH as a catalyst. Toluene, THF, methyl alcohol, and ethyl alcohol were used as solvents. In a standard reaction, 2.5 g of dried PPS (2.74 mmol) was added to a flask equipped with a cooling condenser and a Dean-Stark apparatus. Then 25 ml solvent was added, and then 2.5 wt% KOH based on PPS. The solution was stirred at room temperature under N_2 for 30 min, and then refluxed with stirring for 10 to 200 h. When toluene was used as solvent, a white powder precipitated during the reaction. After the required time, the solution was filtered to recover the powder and the filtered solution was slowly added to hexane to precipitate dissolved product. The precipitated product was filtered, and product washed with hexane. When THF, ethyl and methyl alcohol were used as solvent, the clear solution was also precipitated in hexane, filtered, and product washed with hexane. All samples were vacuum dried at $70^\circ\text{C}/10\text{ h}$.

From mass spectroscopy, GPC, TGA, FTIR, and ^{29}Si NMR analyses, the toluene product that precipitates during the reaction was OPS and the soluble product was PPS. The THF and alcohol reactions gave only PPS. Table 1 shows the effects of solvents and reaction times on the yield and MW of product PPS obtained using 2.5 wt% KOH as catalyst.

The two PPS materials that have different MWs, PPS as-received (low MW PPS) and PPS after polymerization for 200 h in ethyl alcohol (high MW PPS), were used as starting materials to synthesize PAPS. DDPS was also used to prepare DDAPS, and OPS was used for comparative purposes. Selected characterization data of the starting materials are given in Table 2.

2.2.6. Synthesis of polynitrophenylsilsesquioxane (PNPS)

We recently described the nitration and reduction of OPS to make OAPS [30]. The same procedures were used with PPS to make PAPS. Two types of starting materials were

Table 1
Molecular weight and polydispersity of PPS polymerized by reflux with 2.5 wt% KOH in various solvents

Solvent	Reflux time (h)	Yield (%)		MW of PPS measured by GPC		
		PPS	OPS	$M_n (\times 10^3)$	$M_w (\times 10^3)$	(PDI)
Dimeric PPS	–	–	–	1.3	2.2	1.69
Toluene	10	61.2	38.8	1.5	2.3	1.53
	20	55.0	45.0	2.1	3.2	1.52
	100	30.8	69.2	2.0	2.7	1.35
THF	10	59.8	–	1.3	1.7	1.33
	20	62.3	–	1.3	1.7	1.33
	100	66.0	–	1.1	1.3	1.22
Ethyl alcohol	10	65.3	–	4.4	10.3	2.34
	20	69.2	–	5.9	15.3	2.59
	100	71.4	–	18.6	42.9	2.31
	200	75.4	–	24.5	61.0	2.49
Methyl alcohol	10	64.1	–	3.2	8.5	2.65
	20	69.5	–	4.3	10.8	2.51
	100	73.0	–	13.5	33.4	2.47

M_n , M_w , and PDI of OPS are 700, 705, and 1.01, respectively.

used; low MW PPS (M_n : 1.3×10^3) as obtained from Gelest and high MW PPS (M_n : 2.5×10^4) polymerized in EtOH for 200 h. Both reactions were run under the same conditions.

Fuming nitric acid, 30 ml (90%), was added with stirring to a 100 ml flask, and cooled to 0 °C. Then, 5.0 g (4.84 mmol) of PPS was added slowly to the HNO₃ in small portions. After addition, the solution was stirred at 0 °C for 30 min. and further stirred at room temperature for another 20 h. The solution was then precipitated by slowly adding it to 250 g of ice. When the ice melted, the precipitate was collected, washed with water several times to remove acidic components, and vacuum dried at 70 °C/10 h.

The obtained product varied in color: for LMW PPS, a very faintly gray powder (6.09 g, 4.37 mmol, 90%) was obtained, and for HMW PPS, a light yellow powder (6.19 g, 4.44 mmol, 92%) was recovered. All products gave the same analytical data. Both PPSs used as starting materials were soluble in THF, acetone, chloroform, methylene

chloride etc, but all of the obtained PNPS products were soluble in THF, chloroform, acetone, methylene chloride etc. Selected characterization data are given in Table 3.

2.2.7. Synthesis of octa(nitrophenyl)silsesquioxane (ONPS)

The reactions were run under the same conditions as used to make PNPS above. OPS, 5.0 g (4.84 mmol) was added slowly to 30 ml fuming HNO₃ in small portions at 0 °C as done for PNPS. The obtained product was a light yellow powder (6.13 g, 4.40 mmol, 90%), the products gave the same analytical data. OPS was slightly soluble in methylene chloride, but the ONPS product was soluble in THF, chloroform, acetone, methylene chloride etc. Selected characterization data are given in Table 3.

2.2.8. Synthesis of dodeca(nitrophenyl)silsesquioxane (DDNPS)

The reactions were run under the same conditions as used for PNPS above. DDPS, 5.0 g (3.23 mmol) was added

Table 2
Selected characterization data of PPSs as received and after polymerization, OPS and DDPS

Analysis	Low MW PPS	High MW PPS	OPS	DDPS
NMR (ppm)				
¹ H	Ar (8.2–6.4)	Ar (8.2–6.4)	–	–
¹³ C	135.3, 131.9, 129.1	135.5, 132.0, 129.3	–	–
²⁹ Si	–67.4, –76.0	–77.7	–75.9	–74.9, –77.9
FTIR (cm ^{–1})	3725–3290 (Si–OH), 3124–2864 (νC–H), 1597 (νC–C), 1430 (δC–H), 1314–978 (νSi–O–Si), 743 (γC–H), 699 (γC–H)	3120–2835 (νC–H), 1597 (νC–C), 1430 (δC–H), 1307–985 (νSi–O–Si), 743 (γC–H), 698 (γC–H)	3127–2890 (νC–H), 1596 (νC–C), 1432 (δC–H), 1304–990 (νSi–O–Si), 746 (γC–H), 698 (γC–H)	3122–2875 (νC–H), 1596 (νC–C), 1433 (δC–H), 1311–975 (νSi–O–Si), 743 (γC–H), 698 (γC–H)
Ceramic yield (wt%)	46.1 (46.5 ^a)	46.3 (46.5 ^a)	46.1 (46.5 ^a)	45.1 (46.5)
$M_n (\times 10^3)$	1.31	24.52	0.72	0.81
$M_w (\times 10^3)$	2.16	61.00	0.73	0.93
PDI (M_w/M_n)	1.65	2.49	1.02	1.15

^a Theoretical ceramic yield = FW of SiO₂ × 8 (or 12) / FW of PPS (OPS or DDPS) × 100.

Table 3
Selected characterization data of PNPSs, ONPS, and DDNPS, prepared by nitration with fuming HNO₃

Analysis	Low MW PNPS	High MW PNPS	ONPS	DDNPS
NMR (ppm)				
¹ H	7.2–8.8	7.2–8.7	8.7 (t, 1.0H), 8.4–8.7 (m, 4.1H), 7.8 (m, 2.7H)	7.2–8.7
¹³ C	153.6, 151.2, 149.1, 141.1, 139.1, 136.8, 134.5, 133.5, 130.5, 129.9, 127.2, 125.6, 123.9	153.5, 151.3, 150.0, 141.1, 139.0, 136.1, 134.2, 133.3, 131.0, 129.5, 127.0, 125.5, 123.8	154.0, 148.9, 141.0, 138.6, 136.5, 135.3, 134.1, 132.3, 130.8, 129.5, 127.0, 125.2, 123.6	154.2, 149.1, 141.3, 138.6, 137.0, 135.8, 134.0, 132.8, 130.8, 129.6, 127.0, 125.4, 123.8
²⁹ Si	–71.9, –79.8	–79.8	–80.1	–79.9
FTIR (cm ⁻¹)	3183–2861 (ν C–H), 1611 (ν C–C), 1535, 1360 (ν N=O), 1264–987 (ν Si–O–Si), 731, 684 (ν C–H)	3170–2830 (ν C–H), 1609 (ν C–C), 1540, 1360 (ν N=O), 1250–964 (ν Si–O–Si), 737, 502 (ν C–H)	3167–2870 (ν C–H), 1612 (ν C–C), 1535, 1350 (ν N=O), 1268–975 (ν Si–O–Si), 730, 505 (ν C–H)	3166–2872 (ν C–H), 1612 (ν C–C), 1533, 1350 (ν N=O), 1270–978 (ν Si–O–Si), 735, 505 (ν C–H)
Ceramic yield (wt%)	34.2 (34.5 ^a)	34.3 (34.5 ^a)	33.7 (34.5)	33.9 (34.5)
M_n ($\times 10^3$)	1.35	1.80	1.03	1.21
M_w ($\times 10^3$)	1.52	2.20	1.11	1.32
PDI (M_w/M_n)	1.13	1.34	1.08	1.09

^a Theoretical ceramic yield = FW of SiO₂ \times 8 (12) / FW of PNPS (ONPS, DDNPS) \times 100.

slowly to 30 ml fuming HNO₃ in small portions at 0 °C as above. The obtained product was a light yellow powder (6.03 g, 2.88 mmol, 90%). DDPS is slightly soluble in methylene chloride, but DDNPS is soluble in THF, chloroform, acetone, methylene chloride etc. Selected characterization data are given in Table 3.

2.2.9. Synthesis of octaaminophenylsilsesquioxane (OAPS)

ONPS synthesized as above was used as starting material. To a 100 ml Schlenk flask equipped with a condenser and magnetic stirring, was added ONPS (4.0 g, 2.88 mmol) and 5 wt% Pd/C (488 mg, 0.23 mmol). Distilled THF (40 ml) and triethylamine (25 ml, 179.4 mmol) were added under nitrogen. The mixture was heated to 40 °C, and 99% formic acid (3.0 ml, 7.95 mmol) was added slowly at 40 °C under nitrogen with vigorous stirring with a magnetic stir bar. Carbon dioxide evolved with the addition of formic acid and the solution separated into two layers. The reaction was run for 20 h. After the required time, the THF layer was separated from the black slurry by decantation. Then, 60 ml of THF was added to the black slurry and the solution was stirred until a black suspension formed. The suspension and the THF solution were passed through a funnel equipped with a glass fiber/celite filter to remove the catalyst. The two THF solutions were combined. The volume was then reduced to 20 ml under reduced pressure. This solution was put in a separatory funnel with 30 ml of water and 50 ml of ethyl acetate. The solution was washed five times with 250 ml aliquots of water to remove triethylammonium formate by-product and then washed with saturated aq. NaCl (40 ml). The organic layer was then dried over 3 g of Na₂SO₄ to remove water and precipitated by adding into 150 ml of hexane. The precipitate was collected by filtration. The powder was then dissolved in 20 ml of THF and reprecipitated in 150 ml of hexane to remove any remaining triethylamine. The obtained powder was vacuum

dried. The OAPS product obtained from ONPS was very similar giving light yellow powders in 85% (1.41 g 1.22 mmol), and was soluble in THF, acetone etc. Selected characterization data are given in Table 4.

2.2.10. Synthesis of polyaminophenylsilsesquioxane (PAPS)

PNPS synthesized as above was used as the starting material, and the reaction was run under conditions similar to those used to make OAPS above.

To a 100 ml Schlenk flask equipped with a condenser and magnetic stirring, was added PNPS (2.0 g, 1.44 mmol) and 5 wt% Pd/C (244 mg, 0.115 mmol). Distilled THF (20 ml) and triethylamine (18 ml, 129.1 mmol) were added under nitrogen. The mixture was heated to 60 °C, and 99% formic acid (2.09 ml, 55.4 mmol) was added slowly under nitrogen with vigorous stirring. The reaction was maintained at temperature for 5 h and then worked up as used to make OAPS above. The PAPS products obtained from the two different M_n PNPSs were very similar giving light yellow powders in 83% (1.38 g 1.20 mmol) and 84% isolated yield (1.40 g, 1.21 mmol), respectively. All were soluble in THF, acetone etc. Selected characterization data are given in Table 4.

2.2.11. Synthesis of dodeca(aminophenyl)silsesquioxane (DDAPS)

DDNPS synthesized as above was used as the starting material in this reaction and run under the same conditions used to make PAPS above.

DDNPS (2.0 g, 0.84 mmol) and 5 wt% Pd/C (142 mg, 0.096 mmol) were added to a 100 ml Schlenk flask. Distilled THF (20 ml) and triethylamine (13 ml, 83.0 mmol) were added under nitrogen. 99% formic acid (1.83 ml, 40.3 mmol) was added slowly at 40 °C and this reaction was carried out as done to make PAPS above. The DDAPS product was a light yellow powder in 87% isolated

Table 4
Selected characterization data of PAPS, OAPS, and DDAPS prepared by reduction of nitro-functionalized POSS

Analysis		Low MW PAPS	High MW PAPS	OAPS	DDAPS
NMR (ppm)	¹ H	7.8–6.3 (4.0H), 5.2–3.6 (2.0H)	7.9–6.1 (4.0H), 5.2–3.5 (2.0H)	7.8–6.2 (4.0H), 5.2–3.7 (2.0H)	7.8–6.2 (4.0H), 5.3–3.7 (2.0H)
	¹³ C	154.2, 152.0, 148.3, 136.8, 132.8, 129.5, 126.1, 123.8, 121.2, 117.6, 116.0, 114.6	154.1, 151.8, 148.5, 136.5, 132.8, 129.4, 125.9, 123.4, 120.9, 117.5, 115.8, 114.5	154.0, 148.1, 136.6, 132.8, 129.3, 123.4, 120.8, 117.3, 115.8, 114.4	154.1, 151.6, 148.4, 136.7, 132.8, 129.3, 125.8, 123.6, 121.0, 117.5, 115.7, 114.5
	²⁹ Si	–76.0	–76.0	–75.0	–76.7
FTIR (cm ⁻¹)		3360 (ν N–H), 3158–2856 (ν C–H), 1621 (ν C–C), 1441 (δ C–H), 1253–984 (ν Si–O– Si), 698, 498 (ν C–H)	3345 (ν N–H), 3120–2820 (ν C–H), 1600 (ν C–C), 1439 (δ C–H), 1230–970 (ν Si–O– Si), 698, 493 (ν C–H)	3370 (ν N–H), 3150–2820 (ν C–H), 1600 (ν C–C), 1437 (δ C–H), 1230–965 (ν Si–O– Si), 697, 500 (ν C–H)	3353 (ν N–H), 3105–2824 (ν C–H), 1598 (ν C–C), 1437 (δ C–H), 1230–970 (ν Si–O– Si), 697, 495 (ν C–H)
	Ceramic yield (wt%)	41.4 (41.7 ^a)	41.2 (41.7 ^a)	41.1 (41.7 ^a)	41.0 (41.7)
M_n ($\times 10^3$)		1.41	1.62	1.06	1.23
M_w ($\times 10^3$)		1.89	2.34	1.13	1.37
PDI (M_w/M_n)		1.34	1.45	1.02	1.11

^a Theoretical ceramic yield = FW of SiO₂ \times 8 (12)/FW of PAPS (OAPS, DDAPS) \times 100.

yield (1.26 g, 0.73 mmol). It is soluble in THF, chloroform, acetone etc. Selected characterization data are given in Table 4.

2.2.12. Cleavage of Si–C bonds of PNPS, ONPS, and DDNPS

In a 100 ml Schlenk flask equipped with a condenser, was added ONPS (1.0 g, 0.72 mmol), and then tetrabutylammonium fluoride (10 ml) and D₂O (2 ml) were added under nitrogen. The mixture was heated to 70 °C for 24 h. After the required time, Si–O compounds precipitated by the reaction were removed by filtering. The clear filtrate was put in a separatory funnel with 10 ml of ethyl acetate and 10 ml of water. The solution was washed five times with 50 ml aliquots of water to remove by-product, then washed with brine, and the organic layer dried over 1 g of Na₂SO₄ to remove water. The organic solution was removed by rotary evaporation, and the obtained powder was again vacuum dried. PNPS and DDNPS were run the same way. The nitrobenzene obtained from ONPS, PNPS, and DDNPS was a brown liquid in 0.55 (4.47 mmol), 0.51 (4.14 mmol), and 0.53 g (4.31 mmol), respectively. ¹H NMR and GC-MS analyses were used to identify the nitration positions on the phenyl groups.

2.2.13. Peroxide cleavage of Si–C bonds

3.0 g nitrophenylsilsesquioxane, 2.5 g KF, 2.0 g sodium bicarbonate were added to a 250 ml round-bottom flask. 25 ml THF was added and stirred until the silsesquioxane dissolved. Then, 25 ml methanol and 20 ml 30% hydrogen peroxide in water solution was added, whereupon the silsesquioxane precipitated. This mixture was then refluxed for four hours, over which time the solution became clear yellow and later precipitated white silica. The solution was then decanted in order to remove the silica and extracted with ethyl acetate/water three times in order to remove salts. The water layers were combined and extracted with addition ethyl acetate to ensure complete capture of any organic

compounds. The combined organic layers were dried over sodium sulfate and evaporated to remove the solvents. The residual mixture was then analyzed by GC-MS, ¹H-NMR, and ¹³C-NMR as follows. ¹H-NMR: Integration of ¹H-NMR signals of the cleaved product revealed 70% meta, 25% ortho and 5% para. ¹³C-NMR: Peaks indicative of *ortho*, *meta*, and *para* isomers were found, with relative heights consistent with the mol fractions determined by 1H-NMR. MALDI-TOF of uncleaved product revealed substantially pure material, >95% of the signal was indicative of octa-substituted material, with a small amount of hepta-substituted material, incomplete cages, or various adducts.

3. Results and discussion

We have already described the synthesis of OAPS from OPS [30]. The structure of PPS differs from those of OPS or DDPS. OPS and DDPS are a fully-condensed octa- and dodeca-cage structures, respectively, whereas, PPS has an incompletely-condensed framework with reactive Si–OH groups [5].

The M_n , M_w , and PDI of PPS as-received (Gelest) are 1.3×10^3 , 2.2×10^3 , and 1.65, respectively. The MW was lower than expected. Therefore, polycondensation polymerization of the oligomeric PPS was performed to prepare higher MW, to determine if higher MW PAPS materials could be produced. It was assumed that these materials would likely consist of mixtures of partially formed cages. Surprisingly, the resulting materials are all similar and are no longer polymeric but oligomeric.

3.1. Polycondensation polymerization of PPS

Numerous studies on the synthesis of PPS via catalytic hydrolysis and condensation of PhSiCl₃ or PhSi(OR)₃ catalysis have been reported [12–15,31–32]. We briefly studied the same reaction in an effort to prepare high MW

PPS from the Gelest commercial product which is an oligomer.

Thus, low MW PPS as-received was further polymerized by reflux with catalytic (2.5 wt%) KOH in various solvents. The MW of PPS was hardly affected by reaction time in toluene and THF, but, when toluene was used as solvent, with time, the PPS was partially transformed to OPS in a 30:70 OPS:PPS ratio, as shown Table 1. Otherwise, the MW of PPS increased with increasing reaction time in ethyl and methyl alcohol.

The nature of the T units in PPS, silane diol (T_1), silanol (T_2), siloxane (T_3), can be defined by chemical shifts using ^{29}Si -CP-MAS NMR spectra [13–14]. ^{29}Si -CP-MAS NMR spectra of low MW PPS, OPS produced by reflux in toluene, high MW PPS as-polymerized in EtOH, and DDPS are shown in Fig. 1. OPS with perfect cage structures appears as a sharp singlet at -75.8 , whereas, DDPS exhibits broad doublets.

Frye and Collins [34] report that the ^{29}Si NMR spectra of octa- and deca(hydrosilsesquioxane) display singlets indicating the presence of a strain-free structure, whereas dodeca(hydrosilsesquioxane) displays two singlets, peaks with different intensity ratios caused by structural isomers. As-received PPS exhibits two broad peaks at -67.4 ppm (T_2) and -76 ppm (T_3). Thus, this material likely consists of typical 'T' units and bridging silanol groups as suggested by Fig. 1 and based on work by Feher et al. [5]. The broad peak at -67.4 ppm disappears after polycondensation polymerization with KOH in EtOH, and appears as a broad singlet at -77.7 ppm (T_3). The shift of the T_3 peak after polymerization has been suggested to arise because of different environments and molecular weight in the irregular polymer sequences. According to the literature, T unit values shift depending on the method of preparation. The half-height full width (HHFW) values of the T peaks can be used as parameters to analyze the organization of the materials [13–14]. Table 5 shows the position of peaks and HHFW values for PPSs, OPS, and DDPS. OPS and DDPS were also identified by X-ray powder pattern diffraction studies, as crystalline cage structures, whereas the low and high MW PPSs both exhibited amorphous scattering.

Fig. 2 shows FTIR for the PPSs, OPS, and DPPS. In the FTIR, the two PPS starting materials, LMW and HMW PPS, show little difference characterized by two broad maxima associated with $\nu\text{Si-O-Si}$ absorptions in the 1200 – 960 cm^{-1} region. Brown et al. reported that T_{8-12} cages give only one Si-O-Si band at 1120 – 1130 cm^{-1} , while PPS containing open cages and perhaps some ladder structure exhibits two bands at 1135 – 1150 and 1045 – 1060 cm^{-1} [33]. As shown Fig. 3, OPS and DDPS exhibit only single sharp peaks at 1124 cm^{-1} as expected based on the literature. In contrast, the LMW PPS Si-O-Si band appears as a broad doublet in the 1200 – 950 cm^{-1} region, while those of HMW PPS appear sharper and are clearly separated into two peaks at 1126 and 1050 cm^{-1} . On the basis of the FTIR, PPS

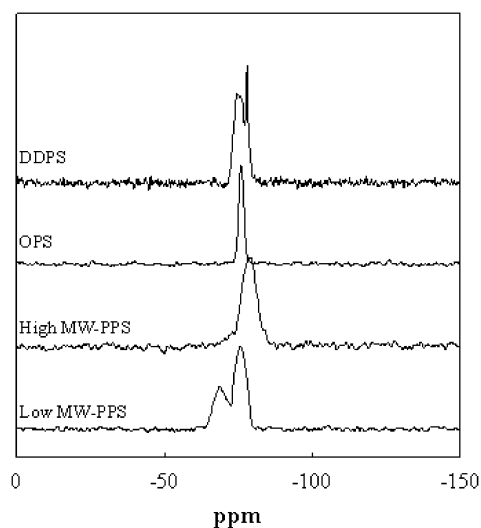


Fig. 1. ^{29}Si -CP MAS solid state NMR spectra on the OPS (a) and high MW PPS (b) obtained by polycondensation of low MW PPS (c) and DDPS (d).

consists of partial cages combined with some ladder content. The ladder content decreases and partial cage structures increase following polymerization. Prado et al. [13] note that PPS FTIR spectra also exhibit bands associated with $\nu\text{Si-OH}$ species. We also see $\nu\text{Si-OH}$ bands at about 3630 cm^{-1} . The broad $\nu\text{Si-OH}$ peak in LMW PPS appears at 3623 cm^{-1} and is not substantially reduced after polymerization. This result agrees with the ^{29}Si NMR data discussed below that supports the existence of Si-OH functional groups.

The two PPS materials, low and high MW PPSs, were used as starting materials to synthesize PAPS. OPS and DDPS were also nitrated and transformed to OAPS and DAPS for comparison. As seen in Tables 1 and 2, they have somewhat different M_n , M_w , PDIs, and structures.

Table 5
The position of peaks and HHFW on PPS, OPS, DDPS, and their derivatives

Materials	Position of peaks (ppm)	HHFW (ppm)
OPS	-75.9	1.8
ONPS	-80.1	3.4
OAPS	-75.0	5.8
DDPS	$-74.9, -79.9$	5.0, 1.2
DDNPS	-79.9	7.5
DDAPS	-76.7	6.5
Low MW PPS	$-67.3, -75.7$	5.5, 6.0
PNPS	-79.8	8.6
PAPS	-76.0	6.0
High MW PPS	-77.7	6.0
PNPS	-79.8	8.5
PAPS	-76.0	6.0

DDPS were obtained from Hybrid-Plastics Inc. and low MW PPS obtained from Gelest co.

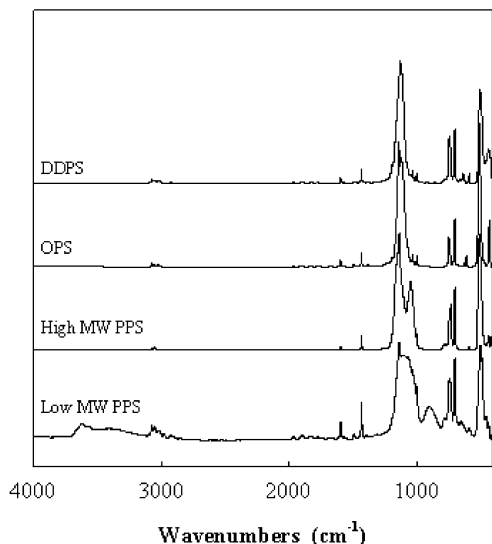


Fig. 2. FTIR spectra on the OPS, DDPS, and high MW PPS prepared by polycondensation of low MW PPS.

3.2. Synthesis of PAPSs, OAPS, and DDAPS

The synthesis of amino-functionalized compounds and oligomers begins with the nitration of the phenyl groups using 90% fuming HNO_3 , followed by reduction of the nitro groups to NH_2 groups. Four starting materials were used; LMW PPS (M_n of 1.3×10^3), HMW PPS (M_n of 2.5×10^4), OPS, and DDPS.

As noted above, the synthesis of OAPS has been described [30] elsewhere. The same procedures were applied to the PPSs, OPS, and DDPS. But, in the reduction of nitro-functionalized POSS, we used milder conditions than previously reported to make OAPS with a nearly perfect cage-structure. Reaction temperatures were reduced to 40° from 60°C , and concentrations of triethylamine and

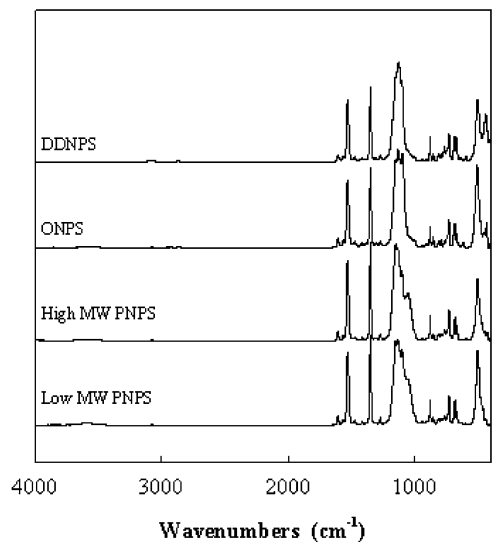


Fig. 3. FTIR spectra on the PNPSs, ONPS, and DDNPS prepared by nitration.

formic acid were reduced. This is because OAPS prepared by the reported procedure [30] contains small amounts of oligomers formed by partial cleavage of the cage-structure during reduction of ONPS. The modified procedures were also used with DDPS to make DDAPS.

The products were characterized by ^1H , ^{13}C , and ^{29}Si NMR GPC, FT-IR, and TGA. ^1H and ^{13}C NMR data for nitro and amino-functionalized products obtained by nitration and reduction with four different starting materials was shown in Tables 3 and 4. All of them are very similar. Broad peak aromatic C–H peaks are observed for PPSs, OPS, and DDPS in the range of 8.2–6.4 ppm. For PNPSs, ONPS, and DDNPS, these peaks are shifted to higher magnetic field, and separate slightly into three peaks because of the substitution pattern on the phenyl groups. For ONPS, the peaks are clearly separated, but not for PNPSs and DDNPS possibly due to more irregular substitution patterns leading to structural isomers, and the structural complexity of PNPSs and DDNPS.

It is essentially impossible to identify the substitution patterns of the nitro groups using ^1H and ^{13}C NMR data. Thus, we ran Si–C cleavage reactions with mixed solvents of tetrabutylammonium fluoride and D_2O to obtain partially deuterated nitrobenzene. The deuterated nitrobenzene was analyzed by ^1H NMR and GC-MS to define positions of nitro groups in ONPS. Also, to aid in these studies we also synthesized octadinitrophenylsilsequioxane (ODNPS), performed a cleavage reaction, and identified the substitution patterns for the isolated dinitrobenzenes.

Generally, considering the electron donating nature of the siloxane group, the introduction of nitro groups was expected to occur mainly in the *meta* position with some *para* without *ortho* substitution. Both the Si–C cleavage reactions of ONPS in $\text{D}_2\text{O}/\text{F}^-$ or by peroxidation to nitrophenols suggest that the nitro groups in ONPS are primarily (70%) attached in *meta* position with substantial amounts (25%) substituted at the *ortho* position and only $\approx 5\%$ in the *para* position. PNPSs and DDNPS were treated similarly with the same results.

In the case of LMW PAPS, HMW PAPS, OAPS, and DDAPS, new peaks appeared at 5.2–3.5 ppm after reduction, which are assigned to N–H protons. The integration ratios of N–H protons to aromatic C–H protons are 1:2.02, 1:1.98, 1:1.94, and 1:1.88, respectively. The number and the position of functional groups in ONPS and OAPS should be the same as expected based on the earlier TGA ceramic yields [30]. The slightly lower ratios found for the oligomeric products may suggest incomplete nitration or some partial double nitration.

Figs. 3 and 4 show FTIR spectra of the nitro- and amino-functionalized materials, respectively. The nitro-functionalized materials exhibit very similar spectra with strong symmetric and asymmetric $\nu\text{N}=\text{O}$ peaks at 1350 and 1530 cm^{-1} . These peaks disappear completely after reduction and new broad $\nu\text{N–H}$ peaks appear in the 3480 – 3320 cm^{-1} range.

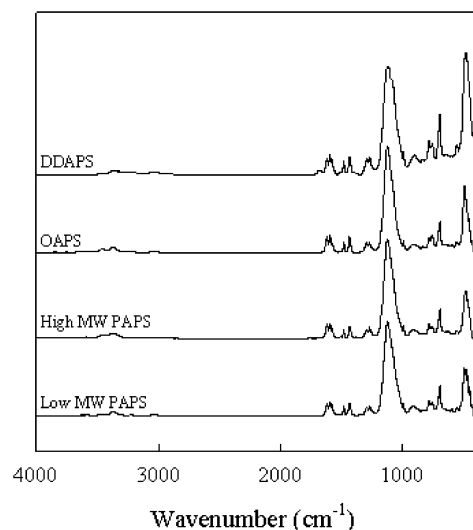


Fig. 4. FTIR spectra on the PAPSs, OAPS, and DDAPS prepared by reduction.

GPC analyses for nitro- and amino-functionalized compounds are shown in Fig. 5 and the effects of reaction temperature on the reduction of ONPS are shown in Fig. 6. As noted above, we previously reported the synthesis of OAPS at 60 °C with Et₃N and formic acid. These conditions result in the formation of unidentified 10–20% oligomeric species presumably by decomposition of the cage structure during reduction. However, the NH:C–H integration remains correct. As shown in Fig. 6 GPC data, reductions at 50 and 60 °C were accompanied with shoulders representing these oligomeric species, but at 40 °C this oligomerization process does not appear to form. Also, we expected to make HMW PNPS and PAPS, but the GPC trace of HMW PPS (M_n of 2.5×10^4) shifts to the low MW region with a shoulder as shown in Fig. 7, making this product look quite similar to the product from the high temperature ONPS reduction products. The M_n and polydispersity are calculated 1.8×10^3 and 1.34, respectively. Thus, it appears

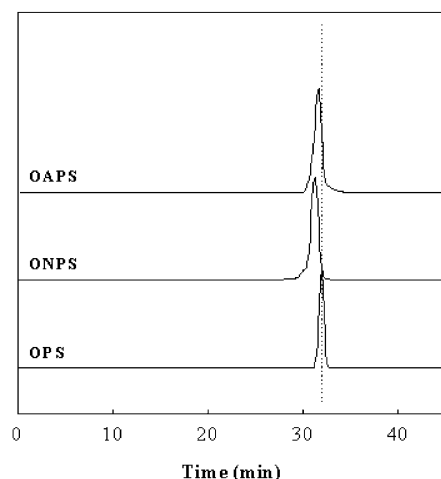


Fig. 5. GPC curves on the ONPS and OAPS.

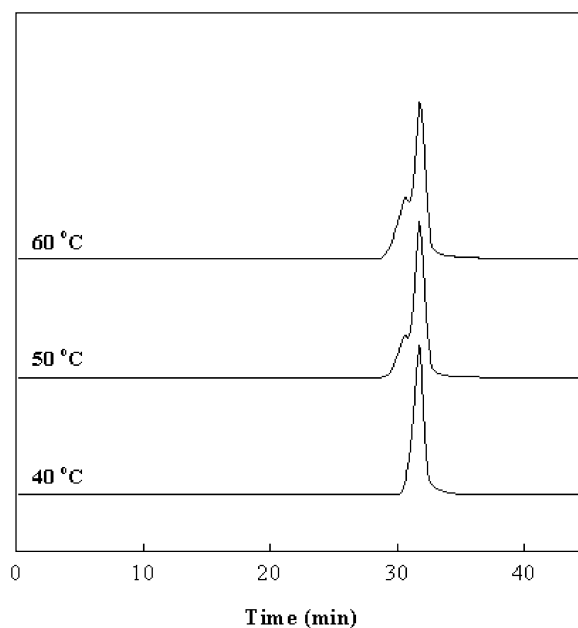


Fig. 6. GPC curves on the OAPSs prepared with three different temperatures in the reduction of ONPS.

that the partial-cage/ladder structure of HMW PPS is cleaved and reorganized by the nitration and reduction processes, which is not unexpected. The M_n suggest that the PAPS is consists of monomer, dimer, trimer species.

In contrast, DDNPS exhibits just a single GPC peak indicating that it survives the nitration process intact. ONPS and DDNPS appear to be very similar in terms of their GPC traces.

Fig. 8 displays the TGAs of high MW PPS, PNPS, and PAPS in air at a ramp rate of 10 °C/min. PPS, which has no functional groups exhibits higher thermal stability than PNPS or PAPS. Both PNPS and PAPS exhibit two-step mass losses. The first loss in PNPS occurs over the range of

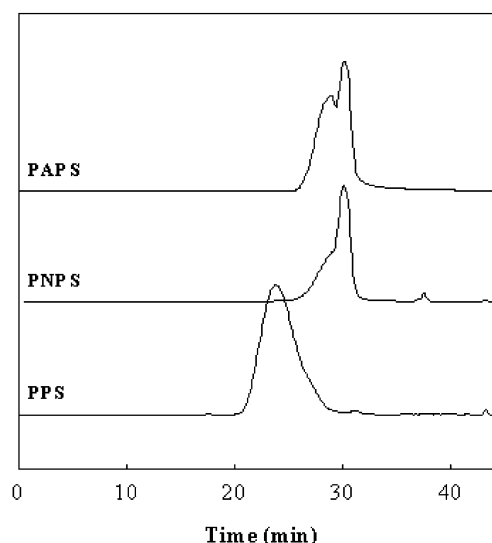


Fig. 7. GPC curves of PPS, PNPS and PAPS.

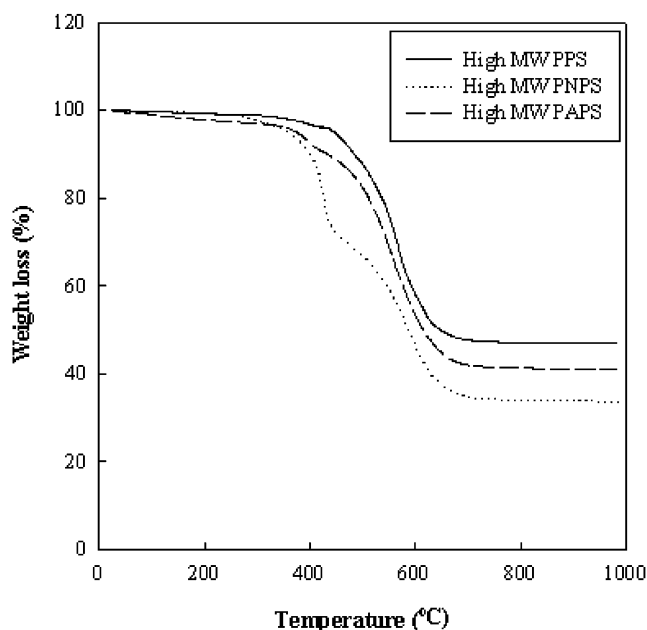


Fig. 8. TGA curves on the PPS, PNPS, and PAPS.

300–430 °C, the mass loss at 430 °C is 22 wt% with the final mass loss at 1000 °C giving a ceramic yield of SiO₂ of 34.2 wt% vs. 34.5 calculated for pure ONPS. These results support the formation of mono-nitrated PPS. Furthermore, they suggest that the loss of phenyl rings during nitration is minimal in the isolated materials. In case of PAPS, the mass loss also occurs via two slightly obscure steps. The first loss at 475 °C is 13 wt% with the final mass loss giving ceramic yields of SiO₂ of 41.0 at 1000 °C. These results support formation of mono-substituted PPS and the conversion of nitro groups to amino groups. The relatively high ceramic yields suggest the loss of some phenyl groups. Nitro- and amino-functionalized phenyl LMW PPS, OPS, and DDPS gave very similar results.

Acknowledgements

We would like to thank the FAA, Pfizer and Guardian Industries for partial support of this work. We would like to thank Mr. Chad Brick for performing the peroxide Si–C cleavage reactions that were so important in defining the substitution patterns.

References

- [1] Voronkov MG, Lavrent'yev VI. *Top Curr Chem* 1982;102:199–223.
- [2] Scott DW. *J Am Chem Soc* 1946;68:356–60.
- [3] Fasce DP, Williams RJJ, Mechin F, Pascault JP, Llauro MF, Petiaud R. *Macromolecules* 1999;32:4757–63.
- [4] Feher FJ, Wyndham KD, Soulivong D, Nguyen F. *J Chem Soc, Dalton Trans* 1999;1491–7.
- [5] Bakhtiar R, Feher F. *Rapid Commun Mass Spectrom* 1999;13:687–94.
- [6] Unno M, Alias SB, Satio H, Matsumoto H. *Organometallics* 1996;15:2413–4.
- [7] Romo-Urbe A, Mather PT, Haddad TS, Lichtenhan JD. *J Polym Sci, Part B: Polym Phys* 1998;36:1857–72.
- [8] Hong B, Thoms TPS, Murfee HJ, Lebrun MJ. *Inorg Chem* 1997;36:6146–7.
- [9] Knischka R, Dietsche F, Hanselman R, Frey H, Mulhaupt R. *Langmuir* 1999;15:4752–6.
- [10] Baney RH, Itoh M, Sakakibara A, Suzuki T. *Chem Rev* 1995;95:1409–32.
- [11] Ladenburg A. *Ber* 1873;6:379.
- [12] Brown JF, Vogt LH, Prescott PI. *J Am Chem Soc* 1963;86:1120.
- [13] Prado LASDA, Radovanovic E, Pastore HO, Yoshida IVP, Torriani IL. *J Polym Sci, Part A: Polym Chem* 2000;38:1580–9.
- [14] Lee EC, Kimura Y. *Polym J* 1998;30:234–42.
- [15] Lee EC, Kimura Y. *Polym J* 1998;30:730–5.
- [16] Ban H, Tanaka A, Kawai Y, Imamura M. *Polymer* 1990;31:564.
- [17] Mi Y, Stern SA. *J Polym Sci, Part B: Polym Phys* 1991;29:389.
- [18] Xie P, Rongben Z. *Polym Adv Technol* 1997;8:649.
- [19] Mine T, Kamasaki S. *Jpn Patent. Kodai-s-60-210570*; 1985. Mine T, Kamasaki S. *Chem Abstr* 1986;104:154450.
- [20] Tsutsui M, Kato S. *Jpn Patent. Kokoku-s-63-20210*; 1988. Tsutsui M, Kato S. *Chem Abstr* 1981;95:192394.
- [21] Feher FJ, Soulivong D, Lewis GT. *J Am Chem Soc* 1997;119:11323–4.
- [22] Feher FJ, Schwab JJ, Soulivong D, Ziller JW. *Main Group Chem* 1997;2:123–32.
- [23] Sellinger A, Laine RM. *Macromolecules* 1996;29:2327–30.
- [24] Sellinger A, Laine RM. *Chem Mater* 1996;8:1592–3.
- [25] Laine RM, Zhang C, Sellinger A, Viculis L. *Appl Organomet Chem* 1998;12:715–23.
- [26] Agaskar PA. *Inorg Chem* 1991;30:2707–8.
- [27] Hasegawa I, Kuroda K, Kato C. *Bull Chem Soc Jpn* 1986;59:2279–83.
- [28] Hasegawa I, Sakka S, Sugahara Y, Kuroda K, Kato C. *J Chem Soc, Chem Commun* 1989;208–9.
- [29] Hasegawa I, Motojima SJ. *J Organometal Chem* 1992;441:373–80.
- [30] Tamaki R, Tanaka Y, Asuncion MZ, Choi J, Laine RM. *J Am Chem Soc* 2001;123:12416–7.
- [31] Frye CL, Klosowski JM. *J Am Chem Soc* 1971;93:4599–601.
- [32] Li GZ, Yamamoto T, Nozaki K, Hikosaka M. *Polymer* 2000;41:2827–30.
- [33] Brown JF, Vogt LH, Prescott PI. *J Am Chem Soc* 1965;87:4317.
- [34] Frye CL, Collins WT. *J Am Chem Soc* 1970;92:5586.